Localized Spot Patterns on the Sphere for Reaction-Diffusion Systems: Theory and Open Problems

Alastair Jamieson-Lane, Philippe Trinh, Michael J. Ward

Abstract A new class of point-interaction problem characterizing the time evolution of spatially localized spots for reaction-diffusion (RD) systems on the surface of the sphere is introduced and studied. This problem consists of a differential algebraic system (DAE) of ODE's for the locations of a collection of spots on the sphere, and is derived from an asymptotic analysis in the large diffusivity ratio limit of certain singularly perturbed two-component RD systems. In [27], this DAE system was derived for the Brusselator and Schnakenberg RD systems, and herein we extend this previous analysis to the Gray-Scott RD model. Results and open problems pertaining to the determination of equilibria of this DAE system, and its relation to elliptic Fekete point sets, are highlighted. The potential of deriving similar DAE systems for more complicated modeling scenarios is discussed.

1 Introduction

Spatially localized patterns can occur for two-component reaction-diffusion (RD) systems in the singularly perturbed limit corresponding to a large diffusivity ratio between the two components in the system. In particular, on the surface of the unit sphere, the stability and dynamics of localized spot patterns, whereby the solution concentrates at discrete points on the sphere, have been analyzed recently for the singularly perturbed Brusselator and Schnakenberg RD systems (cf. [24], [27]). It was also shown that, in certain parameter regimes, these localized patterns can exhibit various instabilities, including either spot-shape instabilities, leading to spot self-

Alastair Jamieson-Lane
Dept. of Mathematics, Univ. of B.C., Vancouver, Canada, e-mail: aja107@math.ubc.ca

Philippe Trinh
OCIAM, Mathematical Institute, Univ. of Oxford, Oxford, U.K e-mail: trinh@maths.ox.ac.uk

Michael J. Ward
Dept. of Mathematics, Univ. of B.C., Vancouver, Canada, e-mail: ward@math.ubc.ca

replication events, or competition instabilities, leading to the annihilation of spots in the pattern. This analysis of [24] and [27] extends the previous studies of localized spot patterns on 2-D planar domains for related RD systems (cf. [6, 11, 29]).

By using formal asymptotic methods on the RD system in the singularly perturbed limit, it is possible to derive a differential algebraic ODE system characterizing the dynamics of spots. This new class of dynamically interacting particle system has some common features with the well-known ODE system characterizing the dynamics of Eulerian point vortices in fluid mechanics. In this latter context, there has been an intense study of the dynamics and equilibria of point vortices on the sphere over the past three decades (cf. [3, 18, 19, 2, 23]). Similar to the original asymptotic derivation of the limiting point vortex problem in [3] starting with the Euler equations of fluid mechanics, the main result for spot dynamics in [27] for the Brusselator and Schnakenberg model, and herein for the Gray-Scott RD model, provides a reduced dynamical system for the time evolution of the centres of the localized spots on the sphere.

Motivated by specific questions related to the development of biological patterns on both stationary and time-evolving surfaces (cf. [5, 20, 12, 17, 21]), there have been many numerical studies of RD patterns on the sphere and other compact manifolds (cf. [1, 13, 14, 28] see also the references therein). Prior analytical studies of RD pattern formation on the surface of the sphere, have focused on using weakly nonlinear and equivariant bifurcation theory to derive normal form equations characterizing the development of small amplitude spatial patterns that bifurcate from a spatially uniform steady-state (cf. [4, 7, 16]). However, as a result of the typical high degree of degeneracy of the eigenspace associated with spherical harmonics of large mode number, these amplitude equations typically consist of a rather large coupled set of nonlinear ODE's. The latter are known to have an intricate subcritical bifurcation structure (cf. [7, 4, 16]). As a result, the preferred spatial pattern that emerges from an interaction of these weakly nonlinear modes is difficult to predict theoretically. This intrinsic difficulty is accentuated for RD systems where there is a large diffusivity ratio, which effectively yields a large aspect ratio system where center manifold analysis is of more limited use [25]. For such large aspect ratio RD systems, there is typically a rather wide band of unstable modes [24, 27], and so the prediction of pattern development based on the conventional paradigm of using both a Turing and a weakly nonlinear analysis is not generally possible.

However, it is in this singular limit of a large diffusivity ratio that localized spot patterns robustly appear from a transient process starting from small random perturbations of a spatially uniform state [24]. A discussion of results and open problems relating to the study of such "far-from equilibrium patterns" is the topic of this short article. In particular, in certain cases the equilibria of this DAE system for spot dynamics have a close relationship to the classical problem in approximation theory of determining a set of elliptic Fekete points, which are the globally minimizer of the discrete logarithmic energy for N points on the sphere.

The outline of this brief article is as follows. In §2, we briefly present the DAE system for the dynamics of spots for the Brusselator models as derived in [27]. In §3 we discuss some results and open questions related to determining equilibria

for these DAE systems. New results for the equilibria of patterns with either 9 or 10 spots are presented. In §4 we give a new result for the DAE dynamics for spot patterns for the well-known Gray-Scott model. Finally, in §5 we list a few open problems related to deriving similar DAE dynamics for spot interactions for more complicated models.

2 Dynamics of Spots on the Sphere

Under the assumption of a large diffusivity ratio and a small "fuel" supply, the Brusselator model of [22] posed on the surface of the sphere, can be scaled into the following system for $u = u(\mathbf{x},t)$ and the inhibitor $v = v(\mathbf{x},t)$ (cf. [27, 24]):

$$\frac{\partial u}{\partial t} = \varepsilon^2 \Delta_S u + \varepsilon^2 \mathrm{E} - u + f u^2 v, \qquad \tau \frac{\partial v}{\partial t} = \Delta_S v + \varepsilon^{-2}\left(u - u^2 v\right), \tag{1}$$

for some $\mathcal{O}(1)$ constants $\mathrm{E} > 0$, $\tau > 0$, and $0 < f < 1$. We refer to E as the "fuel" parameter. Here Δ_S is the Laplace-Beltrami operator on the sphere.

Spatial patterns for which u concentrates as $\varepsilon \to 0$ at a discrete set of points $\mathbf{x}_1, \ldots, \mathbf{x}_N$ on the sphere are called spot patterns. For $\varepsilon \to 0$, we have $u = \mathcal{O}(1)$ in the core of the spot, where $|\mathbf{x} - \mathbf{x}_j| = \mathcal{O}(\varepsilon)$, and $u \sim \varepsilon^2 \mathrm{E}$ away from the spot centers where $|\mathbf{x} - \mathbf{x}_j| = \mathcal{O}(1)$. Then for $\varepsilon \to 0$, the effect of the localized spots on the inhibitor field v in (1) is to introduce a sum of Dirac-delta "forces" where the strength of the "force" induced by the spot at $\mathbf{x}_j$ is proportional to S_j (see [24] for details). As such, v can be represented as a superposition of the well-known source neutral Green's function for the sphere. In this way, in [24] a quasi-equilibrium spot pattern with frozen locations $\mathbf{x}_1, \ldots, \mathbf{x}_N$ was constructed using the method of matched asymptotic expansions by formulating a nonlinear algebraic system for the spot locations $\mathbf{x}_1, \ldots, \mathbf{x}_N$ and the spot strengths $S_1, \ldots, S_N$. The linear stability of this quasi-equilibrium spot pattern to $\mathcal{O}(1)$ time-scale perturbations was analyzed in [24].

Provided that the quasi-equilibrium spot pattern is linearly stable, the slow dynamics of the spot pattern on the long time scale $\sigma = \varepsilon^2 t$ was derived in [27]. The collective coordinates characterizing this slow dynamics are the spot locations $\mathbf{x}_1, \ldots, \mathbf{x}_N$ and their corresponding spot source strengths $S_1, \ldots, S_N$, that both evolve slowly on the long time-scale $\sigma = \varepsilon^2 t$. The slow dynamics derived in [27] is a differential-algebraic system of ODE's as given by the following result:

Principal Result 1 (Slow spot dynamics (cf. [27]))**.** *Let $\varepsilon \to 0$. Provided that there are no $\mathcal{O}(1)$ time-scale instabilities of the quasi-equilibrium spot pattern, the time-dependent spot locations, $\mathbf{x}_j$ for $j = 1, \ldots, N$, on the surface of the sphere vary on the slow time-scale $\sigma = \varepsilon^2 t$, and satisfy the dynamics*

$$\frac{\mathrm{d}\mathbf{x}_j}{\mathrm{d}\sigma} = \frac{2}{\mathscr{A}_j(S_j)}\left(\mathrm{I} - \mathscr{Q}_j\right) \sum_{\substack{i=1 \\ i \neq j}}^{N} \frac{S_i \mathbf{x}_i}{|\mathbf{x}_i - \mathbf{x}_j|^2}, \qquad \mathscr{Q}_j \equiv \mathbf{x}_j \mathbf{x}_j^T, \qquad j = 1, \ldots, N, \tag{2a}$$

coupled to the constraints for $S_1,\ldots,S_N$ in terms of $\mathbf{x}_1,\ldots,\mathbf{x}_N$ given by the roots of a nonlinear algebraic system involving the Green's interaction matrix $\mathscr{G}$

$$\mathscr{N}(\mathbf{S}) \equiv \Big[\mathrm{I}-\nu(\mathrm{I}-\mathscr{E}_0)\mathscr{G}\Big]\mathbf{S}+\nu(\mathrm{I}-\mathscr{E}_0)\chi(\mathbf{S})-\frac{2\mathrm{E}}{N}\mathbf{e}=\mathbf{0}\,. \tag{2b}$$

Here I *is $N\times N$ identity matrix, $(\mathscr{E}_0)_{ij}=\frac{1}{N}$, $(\mathbf{S})_i=S_i$, $(\chi(\mathbf{S}))_i=\chi(S_i)$, $(\mathscr{G})_{ij}=\log|\mathbf{x}_i-\mathbf{x}_j|$ for $i\neq j$ and $(\mathscr{G})_{ii}=0$, $(\mathbf{e})_i=1$, and $\nu=-1/\log\varepsilon\ll 1$.*

From (2) the spot locations are coupled to the spot strengths by (2b), yielding a DAE system for the slow spot evolution. Since the spot strengths can be calculated in terms of the locations from (2b), the DAE system has index 1. One readily established feature of the DAE system (2) is that it is invariant under an orthogonal transformation, corresponding to a rotation of the spots on the sphere.

In this DAE system (2), there are two functions $\chi(S_j)$ and $\mathscr{A}_j(S_j)<0$, which depend only on S_j and the Brusselator parameter f, that must be determined numerically in terms of the local profile of the spot $\mathbf{x}_j$ (cf. [27]). These are shown in Fig. 1 for a few values of f. In the limit $\varepsilon\to 0$, and for $\mathrm{E}=\mathscr{O}(1)$, the only possible $\mathscr{O}(1)$ time-scale instability of the quasi-equilibrium spot pattern is a linear instability of the local spot profile to a peanut-shape if $S_j>\Sigma_2(f)$. This linear instability is found in [24] to lead to a nonlinear spot self-replication event. The threshold values $\Sigma_2(f)$ for spot self-replication for a few values of f are given in the caption of Fig. 1.

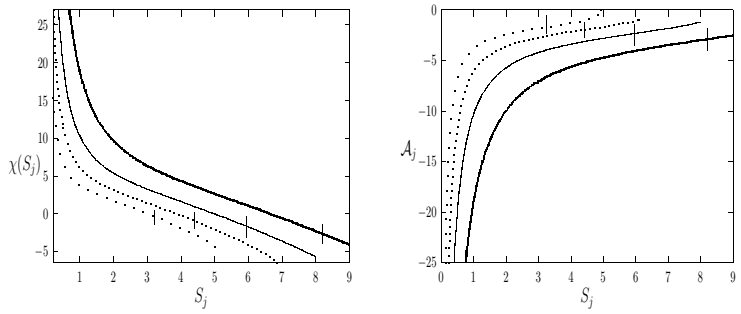

Fig. 1 Left panel: the function $\chi(S_j;f)$ in (2) for $f=0.4$ (heavy solid), $f=0.5$ (solid), $f=0.6$ (dotted), and $f=0.7$ (widely spaced dots). The spot self-replication threshold $\Sigma_2(f)$ for S_j is shown by the thin vertical lines in this figure. If $S_j>\Sigma_2(f)$ the local spot profile is linearly unstable to a peanut-splitting instability (cf. [24]). The threshold values are $\Sigma_2(0.4)\approx 8.21$, $\Sigma_2(0.5)\approx 5.96$, $\Sigma_2(0.6)\approx 4.41$, and $\Sigma_2(0.7)\approx 3.23$. Right panel: the function $\mathscr{A}_j(S_j)<0$ in (2) with the same labels as in the left panel.

3 Equilibria of the DAE Dynamics and Open Questions

In this section we discuss some previous results obtained in [27] as well as some new results for the equilibria of (2) that have large basins of attraction to initial conditions. We consider patterns for small values of N which $S_j = \mathcal{O}(1)$ as $\nu \to 0$. A few open problems are mentioned.

To determine the possible equilibrium spot configurations of (2) with large basins of attraction for $N \geq 3$ when $\mathrm{E} = \mathcal{O}(1)$, f, and ν are given, we performed numerical simulations of (2) for both pre-specified and for randomly generated uniformly distributed initial conditions for the spot locations on the surface of the sphere. To generate N initial points that are uniformly distributed with respect to the surface area we let h_ϕ and h_θ be uniformly distributed random variables in $(0,1)$ and define spherical coordinates $\phi = 2\pi h_\phi$ and $\theta = \cos^{-1}(2h_\theta - 1)$. Newton's method was used to solve (2b) for the initial set of N points. If the Newton iterates failed to converge, indicating that no quasi-equilibrium exists for the initial configuration of spots, a new randomly generated initial configuration was generated. The DAE dynamics (2a) was then implemented by using an adaptive time-step ODE solver coupled to a Newton iteration scheme to compute the spot strengths.

In the simulations below we took $f = 0.5$ and $\varepsilon = 0.02$. We remark that whenever $\mathbf{e} = (1,\ldots,1)^T$ is an eigenvector of the Green's matrix $\mathcal{G}$, then the constraint (2b) admits a solution where $\mathbf{S} = S_c\mathbf{e}$. For such an equal spot–source strength pattern, the equilibrium spatial configuration of spots for (2) is independent of E, f, and ν.

In our discussion below, we refer to a ring pattern as a collection of N equally-spaced spots lying on an equator of the sphere. We refer to an $(N-2)+2$ pattern as a spot pattern consisting of two antipodal spots with the remaining $N-2$ spots equally-spaced on the equatorial mid-plane between the two polar spots.

The simulations of [27] of fifty randomly generated initial spot for $N = 3,\ldots,8$ yielded the following results for equilibria of (2) with large basin of attractions:

- $N = 3$: three equally-spaced spots that lie on a plane through the center of the sphere. (Common spot strength pattern).
- $N = 4$: four spots centered at the vertices of a regular tetrahedron. (Common spot strength pattern).
- $N = 5,6,7$: an $(N-2)+2$ pattern consisting of a pair of antipodal spots, with the remaining $N-2$ spots equally-spaced on the equatorial mid-plane between the two polar spots. (Two different spot strengths for polar and mid-plane spots).
- $N = 8$: a "twisted cuboidal" shape, consisting of two parallel rings of four equally-spaced spots, with the rings symmetrically placed above and below an equator. The spots are phase shifted by 45° between each ring. The perpendicular distance between the two planes is ≈ 1.12924 as compared to a minimum distance of ≈ 1.1672 between neighboring spots on the same ring, so that the pattern does not form a true cube. (Common spot strength pattern).

We remark that for the case $N = 2$ it was shown in Lemma 5 of [27] that any two initial spots on the sphere will become antipodal in the long-time limit $\sigma \to \infty$. This was done by deriving a simple ODE for the angle $\gamma(\sigma)$ between the spot centers $\mathbf{x}_1$

and $\mathbf{x}_2$ at time σ, as measured from the center of the sphere, i.e. $\mathbf{x}_2^T\mathbf{x}_1 = \cos\gamma$, and establishing from this ODE that $\gamma \to \pi$ as $\sigma \to \infty$ for any $\gamma(0)$.

In [27] the linear stability of ring configuration of spots was studied numerically. The following conjecture was formulated in [27] based on numerical experiments.

- A ring pattern of $N = 3$ is orbitally stable, but is unstable if $N \geq 4$.
- For $N = 4, 5, 6, 7$, an $(N-2)+2$ pattern is orbitally stable, but such a pattern is unstable if $N \geq 8$.

More specifically for $N = 3$, the numerical computations of [27] suggest that a ring solution is *orbitally stable* to small random perturbations in the spot locations in the sense that as time increases the perturbed spot locations become colinear on a nearby (tilted) ring. For $N \geq 4$, a similar small, but otherwise arbitrary, perturbation of the spot locations on the ring leads to a breakup of the ring pattern. Similar an $(N-2)+2$ pattern for $N = 8$ breaks up and forms a twisted cuboidal shape.

Open Problem: *Establish analytically these results for the equilibria of spot patterns for $N = 3, \ldots, 8$ using group theory methods for ODE's. Analyze the linear stability of ring patterns by using an approach similar to that done in [2] for the corresponding problem of the linear stability of Eulerian point vortices on a ring.*

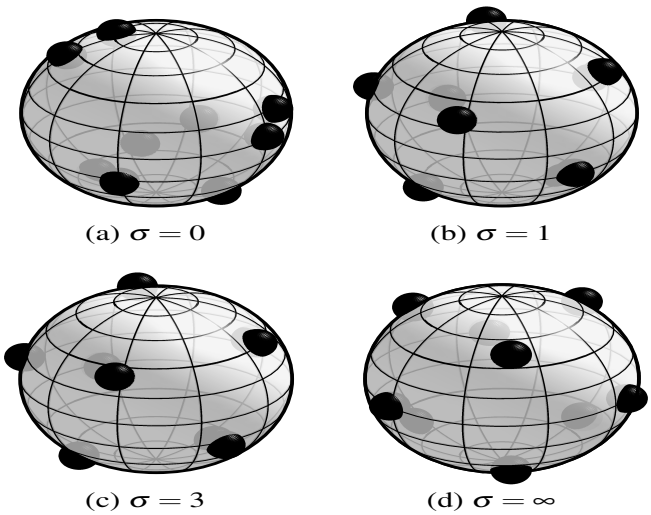

Fig. 2 The evolution of a 9-spot pattern at different time σ for the Brusselator (2) when $f = 0.5$, $E = 18$, and $\varepsilon = 0.02$. Top left: the initial state $\sigma = 0$. Top right: $\sigma = 1$. Bottom left: $\sigma = 3$. Bottom right: the computed steady state after a suitable rotation. The steady-state consists of 3 planes of 3 spots each. The spots on the equatorial plane and the other two planes are phase-shifted 60°. The distance d between the equatorial plane and each of the other two planes is $d \approx 0.7014$. The common value of the spot strengths on the equatorial plane differs from that of the other 6 spots.

For larger values of N it becomes increasingly difficult to visualize the symmetries of the final equilibrium pattern that emerges under the DAE system (2) from initial data. More specifically, it becomes increasingly challenging to find a rotation matrix to put the pattern in a standard reference configuration. We now discuss two new results for $N = 9$ and $N = 10$ not obtained in [27]. For even larger values of N point-matching algorithms from computer science may be useful for classifying the symmetries of the final pattern.

For $N = 9$ the equilibrium state of (2) with a large basin of attraction for initial conditions is the pattern shown in the lower right subfigure of Fig. 2. Our simulations with 50 random initial configurations have shown that the limiting pattern consists of 3 parallel planes of 3 spots each. The spots on the equatorial plane and the other two planes are phase-shifted 60° (see the caption of Fig. 2 for details.)

For $N = 10$ the equilibrium state of (2) with a large basin of attraction for initial conditions is the pattern shown in the lower right subfigure of Fig. 3. The equilibrium pattern consists of two polar spots together with two parallel planes with four equally-spaced spots on each plane. The relative phase-shift of the spots on the two planes is 45° (see the caption of Fig. 3 for details).

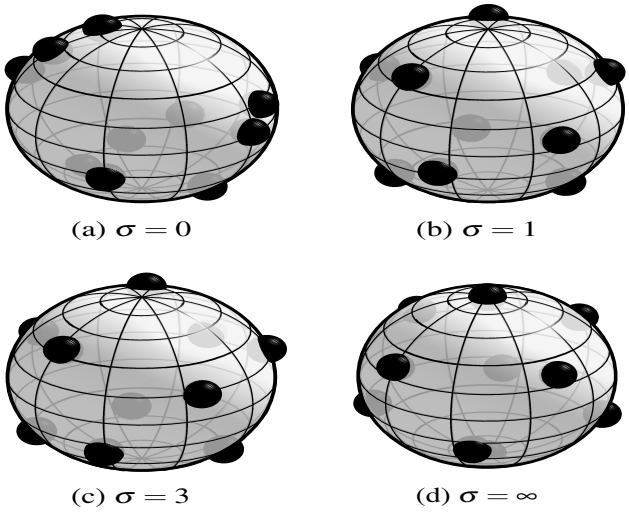

Fig. 3 The evolution of a 10-spot pattern at different times σ for the Brusselator (2) when $f = 0.5$, $E = 22$, and $\varepsilon = 0.02$. Top left: the initial state $\sigma = 0$. Top right: $\sigma = 1$. Bottom left: $\sigma = 3$. Bottom right: the computed steady state after a suitable rotation. The steady-state consists of two polar spots together with two parallel planes of 4 equidistantly spaced spots. The relative phase-shift of the spots on the two planes is 45°. The distance d between the equator and either of the two planes is $d \approx 0.4234$.

A classical problem of point configurations on the sphere is the problem of finding the global minimizer of the discrete logarithmic energy $V \equiv -\sum\sum_{i \neq j} \log |\mathbf{x}_i -$

$\mathbf{x}_j|$ on the sphere where $|\mathbf{x}_j| = 1$. Such optimizing configurations are called elliptic Fekete point sets. By comparing our results for equilibrium spot configurations with the optimal energies V of elliptic Fekete point sets, as given in Table 1 of [26], we conclude that our equilibrium spot configurations for $N = 3, \ldots, 10$ having a large basin of attraction are indeed elliptic Fekete point sets. As a remark, if we were to set $S_j = 1$ in (2) and ignore the constraint (2b), then it is readily seen upon introducing Lagrange multipliers that local and global minima of the discrete energy V are stable equilibria of the simplified DAE dynamics.

Open Problem: *Explore computationally for $N \geq 10$ whether there is a relationship between elliptic Fekete point sets and equilibria of the full DAE dynamics (2) that have large basins of attraction of initial conditions.*

4 Dynamics of Spots on the Sphere: The Gray-Scott Model

In this section we give a new result for the slow dynamics of spots on the unit sphere for the well-known Gray-Scott RD model (cf. [6]).

$$v_t = \varepsilon^2 \Delta_S v - v + Buv^2\,, \quad \tau u_t = D\,\Delta_s u + (1-u) - uv^2\,. \tag{3}$$

Although the analysis of spot dynamics for this problem follows the methodology done in [27] for the Brusselator model, this new analysis requires the reduced-wave Green's function $G(\mathbf{x};\xi)$ on the sphere satisfying

$$\Delta_S G - \frac{1}{D} G = -\delta(\mathbf{x}-\xi)\,, \tag{4a}$$

$$G(\mathbf{x};\xi) \sim -\frac{1}{2\pi}\log|\mathbf{x}-\xi| + R + o(1)\,, \quad \text{as} \quad \mathbf{x}\to\xi\,, \tag{4b}$$

for some R independent of ξ. In terms of this Green's function we can derive the following result for the slow dynamics of a collection of spots for the GS model.

Principal Result 2 (Slow spot dynamics for the GS model)**.** *Let $\varepsilon \to 0$, and assume that $B = \mathcal{O}(\varepsilon/\nu)$, where $\nu = -1/\log\varepsilon$. Then, provided that there are no $\mathcal{O}(1)$ time-scale instabilities of the quasi-equilibrium spot pattern, the time-dependent spot locations, $\mathbf{x}_j$ for $j = 1, \ldots, N$, on the surface of the sphere vary on the slow time-scale $\sigma = \varepsilon^2 t$, and satisfy the dynamics for $j = 1, \ldots, N$,*

$$\frac{\mathrm{d}\mathbf{x}_j}{\mathrm{d}\sigma} = -2\pi\varepsilon^2\gamma_j(S_j)\,(\mathrm{I} - \mathscr{Q}_j)\sum_{\substack{i=1\\ i\neq j}}^{N} S_i \nabla_{\mathbf{x}} G(\mathbf{x}_j;\mathbf{x}_i)\,, \qquad \mathscr{Q}_j \equiv \mathbf{x}_j\mathbf{x}_j^T\,, \tag{5a}$$

coupled to the nonlinear constraints for $S_1, \ldots, S_N$ in terms of $\mathbf{x}_1, \ldots, \mathbf{x}_N$ given by

$$\mathscr{B} = S_j(1 + 2\pi\nu R) + \nu\chi(S_j) + 2\pi\nu\sum_{\substack{i=1\\ i\neq j}}^{N} S_i G(\mathbf{x}_j;\mathbf{x}_i)\,, \quad j = 1, \ldots, k\,. \tag{5b}$$

where $\nu = -1/\log\varepsilon$ *and* $\mathscr{B} \equiv \nu B\varepsilon^{-1}\sqrt{D} = \mathscr{O}(1)$.

In this system $\chi(S_j)$ and $\gamma(S_j)$ depend on the core problem near the spot and are specific to the GS model. Since the reduced-wave Green's function and its regular part R is not available in simple explicit form, and can only be written in terms of the Legendre function (see [24]), it is more challenging to investigate the dynamics and equilibria of spot patterns on the sphere for the GS model. This topic requires further investigation.

5 DAE Spot Dynamics in Complex Models: Open Problems

There are several possible extensions of the methodology for deriving and analyzing localized spot patterns for other scenarios.

We remark that explicit DAE dynamics for spot patterns is only possible when the source-neutral Green's function, satisfying $\Delta_s G = |\Omega|^{-1} - \delta(x - x_0)$ is explicitly available. Such a Green's function is well-known for the sphere, and this fact is key to deriving (2). However, recently in [9], this Green's function has been provided analytically for a particular class of surfaces of revolution. For this class, DAE dynamics on a manifold of varying curvature, and the possibility of pinning of localized spot, can be analyzed.

The second possible extension of the modeling framework is to allow for spatial heterogeneity in the fuel supply, so that $\mathrm{E} = \mathrm{E}(\mathbf{x})$. The corresponding outer solution v will involve a sum of Dirac distributions, one near each spot, together with a term v_p of the form $v_p = \int_\Omega \left(\mathrm{E}(\xi) - \bar{\mathrm{E}}\right) G(x;\xi)\, d\xi$, where $\bar{\mathrm{E}}$ denotes the spatial average of E over the sphere. In this way, it can be shown that the corresponding DAE dynamics will yield a nonlocal system for the evolution of the spots.

Finally, a more intricate method to introduce spatial heterogeneity in (1) is to consider spot patterns on the sphere for a model that couples passive bulk-diffusion in the interior of the sphere to the Brusselator PDE on the surface. In this context, the fuel supply E represents an exchange, or flux, between the surface-bound concentrations and their bulk counterparts. This coupling should lead to rich behavior in the DAE dynamics for spots on the sphere. This paradigm of studying coupled surface-bulk models is becoming more prominent in scientific computation and in applications (cf. [15], [14]).

Acknowledgements PHT thanks Lincoln College, Oxford and the Zilkha Trust for generous funding. MJW gratefully acknowledges grant support from NSERC.

References

1. Barreira, R. Elliott, C.A., Madzvamuse, A.: The surface finite element method for pattern formation on evolving biological surfaces. J. Math. Biol. **6**3, 1095–1109 (2011)

2. Boatto, S., Cabral, H.E.: Nonlinear stability of a latitudinal ring of point vortices on a non-rotating sphere. SIAM J. Appl. Math. **6**4(1), 216–230 (2003)
3. Bogomolov, V.A.: Dynamics of vorticity at a sphere. Fluid Dyn. (USSR). **6**, 863–870 (1977)
4. Callahan, T.K.: Turing patterns with $O(3)$ symmetry. Physica D **1**88(1), 65–91 (2004)
5. Chaplain, M. A. J, Ganesh, M., Graham, I. G.: Spatio-temporal pattern formation on spherical surfaces: numerical simulation and application to solid tumour growth. J. Math. Biology, **4**2(5), 387–423 (2001).
6. Chen, W., Ward, M.J.: The stability and dynamics of localized spot patterns in the two-dimensional Gray-Scott model. SIAM J. Appl. Dyn. Sys. **1**0(2), 582–666 (2011)
7. Chossat, P., Lauterbach, R., Melbourne, I.: Steady-sate bifurcation with $O(3)$ symmetry. Arch. Rat. Mech. Anal. **1**13, 313–376 (1990)
8. Coombs, D., Straube, R., Ward, M.J.: Diffusion on a Sphere with Localized Traps: Mean First Passage Time, Eigenvalue Asymptotics, and Fekete Points. SIAM J. Appl. Math. **7**0(1), 302–332 (2009).
9. Dritschel, D.G., Boatto, S.: The motion of point vortices on closed surfaces. Proc. R. Soc. A **471**, 20140890 (2015)
10. Kidambi, R., Newton, P.K.: Motion of three vortices on the sphere. Physica D **1**16(1-2), 143–175 (1998)
11. Kolokolnikov, T., Ward, M.J., Wei, J.: Spot self-replication and dynamics for the Schnakenberg model in a two-dimensional domain. J. Nonlinear Sci. **1**9(1), 1–56 (2009)
12. Kondo, S. Asai, R.: A reaction–diffusion wave on the skin of the marine angelfish Pomacanthus, Nature, **3**76, 765-768 (1995)
13. Landsberg, C., Voigt, V.: A multigrid finite element method for reaction-diffusion systems on surfaces., Comput. Visual Sci. **1**3, 177–185 (2010)
14. Macdonald, C.B., Merriman, B., Ruuth, S.J.: Simple computation of reaction-diffusion processes on point clouds. Proc. Natl. Acad. Sci. U.S.A., **1**10(23), 9209–9214 (2013)
15. Madzvamuse, A., Chung, A.H.W., Venkataraman. V.: Stability analysis and simulations of coupled bulk-surface reaction diffusion systems. Proc. R. Soc. A **471** 20140546 (2015) :
16. Matthews, P.C.: Pattern formation on a sphere. Phys. Rev. E. **6**7(3), 036206 (2003)
17. Nagata, W., Harrison, L.G., Wehner, S.: Reaction-diffusion models of growing plant tips: Bifurcations on hemispheres. Bull. of Math. Biology **6**(4), 571–607 (2003)
18. Newton, P.K.: The N-vortex problem: Analytical techniques. Springer, New York, (2001)
19. Newton, P.K., Sakajo, T.: Point vortex equilibria and optimal packings of circles on a sphere. Proc. Roy. Soc. A **4**67, 1468–1490 (2011)
20. Painter, K.J.: Modelling of pigment patterns in fish. In: Maini, P.K., Othmer, H.G. (eds.) Mathematical models for biological pattern formation, pp. 58–82 IMA Vol. in Math and its Applications, **121**, Springer-Verlag, (2000)
21. Plaza, R.G., Sánchez-Garduño, F., Padilla, P., Barrio, R.A., Maini, P.K.: The effect of growth and curvature on pattern formation. J. Dynam. Diff. Eq., **1**6(4), 1093-1121 (2004)
22. Prigogine, I., Lefever, R.: Symmetry breaking instabilities in dissipative systems II. J. Chem. Phys. **4**8(4), 1695-1700 (1968)
23. Roberts, G.: Stability of relative equilibria in the planar n-vortex problem. SIAM J. Appl. Dyn. Sys., **1**2(2), 1114-1134 (2013)
24. Rozada, I., Ruuth, S., Ward, M.J.: The stability of localized spot patterns for the Brusselator on the sphere. SIAM J. Appl. Dyn. Sys. **1**3(1), 564–627 (2014),
25. Sewalt, L., Doelman, A., Meijer, H., Rottschafer, V., Zagarias, A.: Tracking pattern evolution through extended center manifold reduction and singular perturbations. Physica D. **2**98, 48–67 (2015).
26. Stortelder, W., de Swart, J., Pintér, J.: Finding elliptic Fekete point sets: Two numerical solution approaches. J. Comput. Appl. Math. **1**30(1-2), 205–216 (1998)
27. Trinh, P., Ward, M.J.: The dynamics of localized spot patterns for reaction-diffusion systems on the sphere. submitted Nonlinearity (39 pages) (2014)
28. Varea, C., Aragón, J.L., Barrio, R.A.: Turing patterns on a sphere. Phys. Rev. E. **6**0(4), 4588–4592 (1999)
29. Wei, J., Winter, M.: Stationary multiple spots for reaction-diffusion systems. J. Math. Biol. **5**7(1), 53–89 (2008).